Cyclic thermomechanical response of fine-grained soil-concrete interface for energy piles applications

Elena Ravera,[1]; Melis Sutman, Ph.D.[2,*]; Lyesse Laloui, Ph.D.[3]

[1]Ph.D. Candidate, Laboratory of Soil Mechanics, Swiss Federal Institute of Technology in Lausanne, Station 18, CH 1015 Lausanne, Switzerland. Corresponding author. Email: elena.ravera@epfl.ch
[2]Postdoctoral Researcher, Laboratory of Soil Mechanics, Swiss Federal Institute of Technology in Lausanne, Station 18, CH 1015 Lausanne, Switzerland.
[*] Assistant Professor, School of Energy, Geoscience, Infrastructure, and Society, Heriot-Watt University, EH14 4AS, UK. Email: m.sutman@hw.ac.uk
[3]Professor, Laboratory of Soil Mechanics, Swiss Federal Institute of Technology in Lausanne, Station 18, CH 1015 Lausanne, Switzerland. Email: lyesse.laloui@epfl.ch

Abstract

Understanding the behaviour of soil-structure interfaces is critical for addressing the analysis and design of energy geostructures. In this study, the interface failure mechanism of energy piles (where a shear band is detached from the surrounding soil that behaves under oedometric conditions) is experimentally analysed in laboratory for saturated conditions. The choice of material (clayey soil and concrete), temperature range, and stress level is based on conditions that are likely to be encountered in practice. Specifically, cyclic thermal tests under constant vertical effective stress in oedometric conditions as well as constant normal stiffness (CNS) interface direct shear tests (in which samples have been subjected to thermal cycles between 10 and 40 °C) are presented. From a practical perspective, the results show very low volumetric strain variations and negligible effects on shear strength. The volumetric aspects do not appear to have significant impact on the shear resistance of the interfaces against cyclic thermal loads. Fundamental insight on the effects of thermal cycles on the concrete-soil interface behaviour which are relevant to energy piles are presented. In addition, the

30   proposed interpretation procedure provides a basis for the standardisation of

31   thermomechanical testing in geotechnical engineering.

32   **Keywords:** energy piles, soil-concrete interface, thermomechanical behaviour,

33   laboratory testing, cyclic load.

1. Introduction

35   In geotechnical engineering, the study of non-isothermal soil behaviour dates

36   back to the 1950s and 1960s. During that time, the focus was on understanding the

37   effects of temperature on engineering properties, generating thermal pressurisation

38   for saturated soils, and soil sampling. From the 1970s to the 1990s, several new

39   geotechnical applications that required understanding of the behaviour of soils

40   subjected to temperature changes (e.g., design in permafrost regions, nuclear

41   waste storage, buried high voltage electrical cables) were introduced. Most of the

42   available research and literature that started in those years and developed until

43   more recent times focuses mainly on the design of repositories for radioactive

44   waste disposal in deep geological media and the consequent development of

45   advanced thermo-hydro-mechanical constitutive models to provide long-term

46   nuclear waste management solutions (e.g., Laloui et al. 2008). Starting from the

47   2000s, there has been an interest in environmentally friendly technologies capable

48   of addressing climate change challenges, such as energy geostructures and other

49   thermoactive ground structures (McCartney et al. 2019; Laloui and Rotta Loria

50   2019). Understanding the behaviour of soil-structure interfaces is critical to

51   address the analysis and design of energy geostructures, e.g., the analysis of

52 energy pile capacity subjected to cyclic thermal loads. As a result of their

53 multifunctional roles, energy piles are exposed to daily and seasonal temperature

54 variations during their lifetime. Therefore, possible effects of cyclic thermal load

55 need to be investigated, e.g., thermal effects resulting in volumetric response of soil

56 at the pile–soil interface at different temperatures, as well as mechanical effects

57 (i.e., displacements at the interface) resulting from cyclic axial dilation and

58 contraction of the concrete during heating and cooling. Both may affect the normal

59 stress at the soil-pile interface which may lead to changes in the soil-pile shear

60 resistance.

61 The analysis presented in this paper reproduces the interface failure mechanism

62 of energy piles in the laboratory for saturated conditions. A schematic

63 representation of the failure mechanism of the pile-soil interface which consists of

64 large localised strains concentrated in a thin layer around the pile, i.e., the

65 interface, is shown in Figure 1. Figure 1 also illustrates the modelling approach

66 adopted in the laboratory to reproduce the failure mechanism where a shear band

67 is detached from the surrounding soil that behaves under oedometric conditions.

68 The presence of the surrounding soil is replicated by a spring stiffness which

69 accounts for the effects of the volume changes (i.e., normal stress variations).

70 Therefore, the basic aspects that constitute the failure mechanism, i.e. the

71 volumetric response of the soil, under oedometric conditions, and the shear

72 response of the soil-concrete interface to cyclic thermal loads need to be

73 addressed individually and combined to fully describe and better understand the

74 failure mechanism at the pile-soil interface.

75   For this purpose, a critical overview of the current framework adopted for

76   analysing phenomena related to the thermovolumetric behaviour of fine-grained

77   soils and the thermomechanical behaviour of interfaces is first presented in the

78   respective introductory sections. The study then focuses on the response of fine-

79   grained soils and soil-concrete interfaces for energy piles applications where

80   drained conditions are assumed upon thermal loading (Mimouni and Laloui 2015;

81   Sutman 2016; Rotta Loria and Laloui 2017a) and temperature values are between

82   2 and 45 °C (Laloui and Rotta Loria 2019). The experimental programme aims to

83   investigate the thermomechanical effects on the response of fine-grained soils and

84   soil-concrete interfaces subjected to cyclic thermal loads. The choice of material,

85   range of temperature, and applied stresses is based on the conditions that are

86   likely to be encountered in practice. Specifically, cyclic thermal tests under

87   constant vertical effective stress in oedometric conditions with temperatures

88   ranging between 10 and 40 °C have been conducted to study the volumetric

89   response of fine-grained soils. The focus on this type of material is based on their

90   historically observed higher sensitivity to temperature variations compared to

91   coarse-grained soils. The purpose is to discuss the influence of cyclic thermal

92   loads on the material under consideration. In interface analysis, changes in

93   volumetric response mean changes in boundary conditions. Moreover, constant

94   normal stiffness (CNS) direct shear tests, in which the soil-concrete interface has

95   been subjected to thermal cycles, are presented. The constant normal stiffness

96   condition has been adopted to account for the effects of the volume changes that

97   occur when the soil adjacent to the pile is sheared (Tabucanon et al. 1995). Spring

98   stiffness is used to replicate the presence of the surrounding soil, which partially

99 prevents the volumetric response. Consequently, the normal stress acting on the

100 interface may increase or decrease because of the dilative-contractive behaviour at

101 the pile-soil interface (Fakharian and Evgin 1997). The purpose is to analyse the

102 response of the interfaces between fine-grained soils and concrete to cyclic

103 thermal and mechanical loads and the effects on shear strength. Finally, the

104 combination of the volumetric and shear aspects aims to better represent and

105 understand the fundamental failure mechanism at the soil-concrete interface.

2. Thermovolumetric behaviour of fine-grained soils

107 Although the first studies on the effects of temperature on the engineering

108 behaviour of soils date back to the 50s and 60s (see the historical perspective

109 provided by Laloui and Cekerevac 2003; McCartney et al. 2019), some of the

110 mechanisms of thermal volume change remain to be understood. The lack of

111 information about loading sequences is one of the main causes that prevent

112 complete understanding. In many studies, details on the thermal and mechanical

113 history of the material did not receive adequate attention (Hueckel et al. 2009).

114 Particularly, the drainage conditions under which heating was performed were not

115 discussed in depth and the time dependency on thermal consolidation was not

116 considered (Coccia and McCartney 2016). Variations in procedures lead to

117 varying outcomes and therefore, observations of studies targeting different

118 applications are difficult to compare. Indeed, the results of each test depend

119 primarily on how the test is performed (Laloui et al. 2014).

120 Based on both the pioneering work of Campanella and Mitchell (1968) and the

121 critical analysis presented by Coccia and McCartney (2016), the current

framework identifies three possible mechanisms responsible for the thermal

volume change of saturated soils. The first mechanism, thermal primary

consolidation, is associated with a time-dependent volumetric contraction of the

soil as the pore water pressure generated by the increase in temperature dissipates.

Water in the pores of soil matrices has a thermal expansion coefficient

approximately 7–12 times greater than that of the solid particles. This generates

pore water pressure within the soil, if heated in undrained or drained conditions,

for fine-grained soils. In the latter case, a temporary undrained condition is

induced as the drainage is usually delayed because of the relatively low

permeability of the soil. Therefore, the heating rate and soil permeability are the

two predominant factors that govern and influence this thermal volume change

mechanism. The second mechanism, thermal secondary compression, is

associated with particle rearrangement. Current studies have sought to explain this

phenomenon by assuming that physicochemical interactions govern the processes

at the microscale. Campanella and Mitchell (1968) suggested that a decrease in

the shear strength of inter-particle contacts occurs as temperature increases and

that this phenomenon should end when new bonds are developed to carry the

induced stresses. In addition, according to Laloui and Rotta Loria (2019), the

physicochemical interactions contributing to this phenomenon appear to be (i) the

degradation of the adsorbed water layer caused by an increase in temperature

(Fleureau 1979; Pusch 1986), (ii) the variations in the rigidities of the mineral

involved, which modify the contact force network (Kingery et al. 1976), and (iii)

the modifications of the equilibrium between the Van der Waals attractive forces

and the electrostatic repulsive forces (Laloui 2001). However, these theories lack

146   experimental observations; thus, they remain unproven. The third mechanism is

147   related to the variation of water viscosity with temperature. An increase in

148   temperature results in a decrease in pore water viscosity. This mechanism is

149   considered to have both the ability to enhance the drainage and to accelerate the

150   thermal secondary compression (Coccia and McCartney 2016).

151   Based on the described traditional framework, the literature links the thermally

152   induced deformation of fine-grained soils mainly to one of these three

153   mechanisms. Finn (1951), Plum and Esrig (1969), Towhata et al. (1993), Romero

154   (1999), Abuel-Naga et al. (2007), and Vega et al. (2012) performed tests in which

155   the heating phase was undrained or incompletely drained (leading to excess pore

156   water pressure generation). Pore water pressure dissipation was allowed after the

157   thermal equilibrium was established. In these cases, the thermal volume change

158   was mainly associated with the effects of pore water dissipation. In the tests

159   conducted by Campanella and Mitchell (1968), Baldi et al. (1991), Hueckel and

160   Pellegrini (1996), and Cekerevac and Laloui (2004), the volumetric strain of the

161   soils during the drained heating was calculated based on the volume of water

162   expelled from the saturated samples. In all these cases, the observations were

163   made when the temperature T stabilised (i.e., $T=const$ over time). Therefore, the

164   deformations observed after heating were attributed to the rearrangement of

165   particles. Soil skeleton rearrangement resulted from allowing the samples to be

166   maintained at a constant temperature after a change in temperature occurred; thus,

167   it was more related to the long-lasting action of the heat on the clay. Furthermore,

168   more recent studies have related thermal consolidation with thermal secondary

169   compression (Di Donna and Laloui 2015; Shetty et al. 2019). Burghignoli et al.

7

(2000) considered the deformations observed after heating as an amplification of those related to creep deformation of the soil skeleton at a constant temperature. This concept of "thermally accelerated creep" was also revived by Coccia and McCartney (2016), where the volume changes were attributed to the variation in pore water viscosity with temperature. Therefore, it refers to the third mechanism originally proposed by Paaswell (1967).

Nevertheless, attributing the volumetric response to a single mechanism is not sufficient for describing this phenomenon completely. Gaps and contradictions persist in each of them. Logically, all mechanisms are considered to contribute to the observed global response; additionally, the prevalence of one mechanism over another depends on the load history to which the sample is subjected. Moreover, the time factor, both in the heating rate adopted and in the interpretation of the consolidation curve, plays a decisive role.

One of the main challenges at the macroscopic scale (i.e., when soil is idealised as a superimposed continua) is the relative role of primary consolidation and secondary compression in the volumetric response of fine-grained soils (Rotta Loria and Coulibaly 2020). Special attention has been devoted to this issue in the interpretation phase of the experimental results of this study. In addition, by focusing on energy piles, the current knowledge is mainly based on lessons learned from research on other applications (mainly nuclear waste storage) and there are therefore some differences in the stress paths to which the sample should be exposed, such as the cyclic variations (heating and cooling) and temperature ranges investigated. Recently, Di Donna and Laloui (2015) made efforts in this direction; however, there are still few experimental results to date. All these

194 aspects, as well as the time dependency, require further understanding and have

195 therefore been addressed in this study.

2.1 Experimental investigation in oedometric conditions

197 This section aims to present several experimental results that are significant for

198 the application of energy piles, focusing on the engineering aspects of the

199 thermomechanical behaviour of fine-grained soils.

200 Thermovolumetric behaviour is studied through oedometric tests. Temperature

201 variations are cyclic and cooling phenomena are involved; they occur in drained

202 conditions. Moreover, an interpretation procedure based on mechanical analogy is

203 proposed, in which the time dependency of the thermal consolidation is

204 considered. The following sections provide details on the apparatus, sample

205 preparation, and experimental procedures adopted in the tests.

2.1.1 Materials and method

207 *Materials*

208 A clayey soil with a mineralogical composition of 77% illite, 10% kaolinite,

209 12% calcite, and traces of feldspar and quartz was used in the experiments. At

210 laboratory conditions (Temperature, $T = 20$ °C), the clayey soil had a liquid limit

211 of 56%, plastic limit of 32%, plasticity index of 24%, and specific gravity of 2.65.

212 The particle size distribution is shown in Figure 2.

213 The clay was maintained in the laboratory in powder form with a hygroscopic

214 water content of approximately 5%.

215 *Sample preparation*

216 A hydraulic press (Wykeham Farrance Eng. Ltd.) was used to prepare the

217 samples via static uniaxial compaction. The press was equipped with a load cell

218   (BLH U3G1, maximum vertical force 22 kN, accuracy 1 N) and a linear variable

219   differential transformer (LVDT) (HBM W 10 TK, accuracy 1 μm). The air-dried

220   powder under laboratory conditions was mixed with the required amount of water

221   to achieve an initial water content of 36%. The mixture was stored in airtight

222   containers for at least three days for moisture equilibration. For the compaction,

223   the soil mass was confined in a rigid mould, and a variable static force was

224   gradually applied through the movement of a piston in the strain-controlled press,

225   until the desired dry density of 1.10 Mg/m^3 was reached. The setup was designed

226   to keep the water content constant during the compaction. This corresponds to a

227   process of compressing a partially saturated sample under undrained conditions.

228   The compaction velocity was controlled through the motor of the machine, at a

229   piston travel rate of 0.5 mm/min. The maximum vertical compaction stress was 82

230   kPa. After compaction, the samples were trimmed down in the corresponding

231   oedometric ring. A height of 45 mm (corresponding to three oedometric samples,

232   being the height of the oedometric ring 15 mm) was chosen to allow two samples

233   to be prepared simultaneously. Parallel tests were conducted to ensure

234   repeatability of the results. The remaining material was used for water content

235   control. At this stage, size and weight measurements of the samples were recorded

236   to determine the initial conditions.

237   *Equipment*

238   The clayey soil was tested in specially designed temperature-controlled

239   oedometric cells (Figure 3). The experimental setup was developed by Di Donna

240   and Laloui (2015); it consisted of various oedometric cells equipped with a

241   hydraulic temperature control system. Each cell was heated using a spiral tube

242   positioned around the sample, through which water was circulated at the desired

243   temperature. The hydraulic circuit was connected to a thermal bath, which had the

244   dual function of maintaining the temperature and introducing water into the

245   system using a pump. This system allowed for heating and cooling cycles to be

246   performed. The delay and the difference in temperature between the thermal

247   variation in the heating system and the real temperature change within the sample

248   were assessed during the calibration process. For this purpose, the relationship

249   between the imposed temperature and the temperature inside the cell was carefully

250   determined using a series of thermocouples (Thermocoax type K, Chromel-

251   Alumel, 2AB 35 DIN, resolution 0.01 °C). Thermal losses were minimised by

252   using a polystyrene box as an insulating system around the cells. In addition, the

253   equipment was carefully calibrated to assess the deformability of the cells under

254   thermal and mechanical loads. The vertical displacement of the sample was

255   measured using an LVDT (HBM W 10 TK, accuracy 1 μm), which had to account

256   for the deformation of the device. To correct the measured vertical displacement,

257   a steel sample with a known linear thermal expansion coefficient and Young's

258   modulus was used during the calibration tests. The oedometric conditions were

259   ensured using an invar oedometric ring which guarantee the minimisation of

260   thermal radial deformation. During the calibration tests, the same loading paths

261   and configuration adopted subsequently in the real tests were applied. Finally,

262   saturation conditions were maintained using a water supply system that

263   compensated for water evaporation.

264   *Experimental programme*

The experimental campaign aimed to characterise the cyclic thermovolumetric response of clayey soils by applying stress paths representative of the real conditions of the soil in situ when an energy pile foundation is in operation. It consisted of saturated oedometric tests, in which thermal cyclic loads were applied under a constant mechanical load. Temperature and vertical stress were the two variables controlled during the tests; the imposed values of these variables were defined based on the operating ranges of the energy piles.

The experimental work included three types of tests involving heating-cooling cycles at different constant vertical stresses and different overconsolidation ratios (OCRs). For each type of test, two samples were tested in parallel to ensure repeatability of the results. Standard oedometric tests were performed to characterise the material. Table 1 provides a summary of the variables that distinguish the tests. Figure 4 shows the thermomechanical paths of the tests. Regarding the mechanical load, the consolidation was performed following the ASTM D2435/2435M-11 standard. The saturation phase was performed by flushing the sample without back pressure saturation. Although according to the ASTM D2435/2435M-11 standard, inundation of the test sample is not always a guarantee of achieving complete saturation, the final degree of saturation was computed to be approximately 90% or higher in all the tests. Therefore, a quasi-saturated state was achieved in all the tests. During the initial saturation phase, the sample was allowed to swell. Nonetheless, the initial void ratio was preserved, considering the low swelling potential of the material. Table 2 shows the initial conditions of the samples after the saturation phase. After saturation, the tests were conducted in two distinct stages. In the first stage, a conventional

289   mechanical consolidation was performed where load increments of constant total

290   axial stress were applied to the sample until a target vertical stress was reached. In

291   the second stage, drained heating-cooling cycles were performed. Five (i.e., 15

292   days) and two (i.e., 6 days) complete heating-cooling cycles were conducted for

293   Test 1, and Test 2 and 3, respectively. The temperatures investigated were in the

294   T=10÷40 °C range. Attention was paid to heating and cooling rates to avoid the

295   generation of significant excess pore water pressure at a rate of 2.0 °C/h.

296   Observations from previous in-situ tests (Mimouni and Laloui 2015; Sutman

297   2016; Rotta Loria and Laloui 2017a) highlighted that the temperature changes

298   induced in the soil occurred in drained conditions.

2.1.2 Test results

300   One of the challenges of testing under non-isothermal conditions is the lack of

301   standards and interpretation procedures, making it difficult to compare results

302   among different studies.

303   In this section, the proposed procedure is based on the analogy of the

304   consolidation process caused by pressure changes and thermal variations

305   (Campanella and Mitchell 1968). In the context of energy piles, this approach is

306   convenient because it allows analysing the effects of mechanical and thermal

307   loads for the design of a foundation, according to the classic scheme of

308   geotechnical analysis.

309   In one-dimensional incremental mechanical loading tests, the experimental data

310   represent a consolidation, partly resulting from the dissipation of pore water

311   pressure (generated by the applied load) and partly from creep phenomena. For

312   this analysis, only the consolidation corresponding to the dissipation of pore water

313   pressure (i.e., primary consolidation) is of interest. This is defined in time-

314   deformation curves typically using the Log Time Method, where it is identified as

315   the intersection of two straight lines; the first made tangentially to the inflexion

316   point and the second coinciding with the final part of the experimental curve. An

317   alternative procedure is to use the Square Root of Time Method.

318   A similar interpretation procedure for the thermal load is shown in Figure 5. A

319   normally consolidated (NC) soil sample is first heated in drained conditions (i.e.,

320   2 °C/h for 10 increments). At each temperature increment, the sample initially

321   dilates owing to the thermal expansion of the soil constituents. Drainage is usually

322   delayed because of the relatively low permeability of the clay and the impedance

323   effects of the ceramic disc (Campanella and Mitchell 1968; Romero 1999). After

324   ten increments (i.e., for approximately every 20-degree increase in temperature),

325   the excess pore water pressure was allowed to completely dissipate, keeping the

326   temperature constant for a prolonged time. Figure 5a shows the intersection of the

327   two straight lines, identified based on a procedure similar to that used in the

328   mechanical case, corresponding to the end of the primary consolidation. Evidence

329   shows that, given a drained thermal increase, the primary consolidation is

330   minimised as attention was placed to avoid creating excessive pore pressures in

331   the sample; additionally, most of the thermal consolidation is associated with the

332   secondary compression. This result agrees with the observations made by

333   Campanella and Mitchell (1968), Burghignoli et al. (2000), Shetty et al. (2019),

334   according to which the deformations are mainly attributed to secondary

335   compression. Soil skeleton rearrangement results from allowing the sample to

336   remain at constant temperature after a temperature change. Therefore, it is related

14

337　to the long-duration effects of heat on clay. Thermal primary consolidation

338　becomes more important for the low permeability and high heating rate because of

339　the higher pore pressure generation. Figure 5b shows the same interpretation

340　procedure adopted for the 5th cycle. Notably, the primary consolidation and

341　secondary compression can be recognised as in the first cycle. In this case, the

342　secondary compression is almost negligible as particle rearrangement already

343　occurred in the first cycles and a stable configuration of the solid particles is

344　progressively reached. Figure 6 shows the same features of Figure 5, but for an

345　over consolidated (OC) clay. In OC conditions, the available space for inducing

346　additional collapse is reduced compared to NC conditions. Therefore, the particle

347　rearrangement is limited. In this case, as expected, the secondary compression did

348　not occur in the first cycle due to the soil structure being more stable.

349　　During the cooling phase, the constituents contract leading to a stable

350　configuration of the solid particles; thus, as a result of this phase, there is no

351　rearrangement of the particles for neither NC nor OC clays.

352　　The main observation is that cyclic loads contribute more to primary

353　consolidation as temperature changes are continuous over time. The effect of pore

354　pressure generation and dissipation on the volumetric behaviour depends on

355　factors such as the heating-cooling rate and permeability of the soil. Secondary

356　compression, however, is attributed to the presence of an elevated temperature (in

357　the case of heating) for extended periods. This can be recognised as an indirect

358　effect of cyclic loads. Different ground temperatures than the initial temperature

359　result from unbalanced heating and cooling cycles. Indeed, cycle imbalance can

360　lead to an average ground temperature that deviates from the initial one in the

361 long term. Therefore, the long-lasting effects must be considered in the long-term

362 design. In this regard, the work of Campanella and Mitchell (1968), Baldi et al.

363 (1991), Hueckel and Pellegrini (1996), and Cekerevac and Laloui (2004), in

364 which observations of volumetric strain with temperatures referred to a condition

365 in which the temperature stabilised and remained constant for an extended period,

366 are useful. In addition, temperature increases may influence time-dependent

367 effects such as creep (Leroueil and Soares Marques 1996; Mitchell and Soga

368 2005; Laloui et al. 2008).

369 　The results of this study focus primarily on the effects of cyclic thermal loads.

370 Therefore, the points shown in Figure 8 identify the deformations of the sample

371 resulting from the thermal load at the end of the primary consolidation, as

372 commonly reported in the oedometric curves interpreted according to the method

373 of Casagrande or Taylor for mechanical loads. The standard oedometric results,

374 which refer to Test 0, are shown as an example in Figure 7. Notably, although the

375 loading process is to be considered drained in the case of fine-grained soils,

376 drainage is usually delayed because of the relatively low permeability

377 (Campanella and Mitchell 1968). Therefore, it is possible to distinguish the

378 primary consolidation (in this case reduced to a minimum given the drained

379 loading process) and the secondary compression (as explained in the previous

380 paragraph concerning Figures 5 and 6). Based on the results in Figure 8, which

381 refer only to the primary thermal consolidation, very low residual strain variations

382 are observed within the temperature range analysed. During temperature cycles

383 (i.e., temperature variations) the soil components expand when heated and

384 contract when cooled leading to very small residual strain. The phenomenon is

observed both in samples under NC (Figure 8a) and OC conditions (Figure 8c). In the case of higher confinement (i.e., 1000 kPa), the behaviour is also similar for the temperature ranges analysed (Figure 8b). However, a greater tendency to contract at the end of the primary consolidation is observed, which is attributed to the increase in pore pressure owing to lower porosity. Comparison between mechanically induced axial strain (Figure 7) and thermally induced axial strain (Figure 8), associated with the operation of the energy piles, highlight that the latter is significantly small (2-3 order of magnitudes smaller than mechanical ones). Although residual thermal strain variations have been observed, these appear to be small and negligible from a practical perspective. Therefore, the assumption of a reversible behaviour may be justified in analysis approaches for energy piles.

Multiple tests were conducted in parallel under the same conditions to ensure the repeatability of the phenomena.

The interpretation presented may serve as a basis for a future standardisation process of thermomechanical tests in geotechnical engineering. The contributions of these experimental results add knowledge on the thermovolumetric behaviour of fine-grained soils and provide an answer on how the soil behaves with a focus on cyclic loads. Usually, this is sufficient for resolving geotechnical issues. More fundamental questions related to the description of microscale processes (i.e., physicochemical processes that occur in the soil at the particle level) that influence macroscopic behaviour are not addressed in this study.

Based on these results, it is possible to make some considerations for the analysis and design of energy piles and highlight how neglecting the temperature

409 sensitivity of the volumetric behaviour of the soil may be justified, e.g., using

410 simplified analysis approaches (Rotta Loria and Laloui 2016, 2017b; Sutman et al.

411 2019; Ravera et al. 2020a, 2020b). In addition, considering these results, when

412 analysing the soil-concrete interface failure mechanism, reversible volumetric

413 deformations imply that the boundary conditions of the interface are not affected

414 by the temperature cycles.

3. Thermomechanical behaviour of the fine-grained soil-concrete interface

417 An effective stress approach for both coarse- and fine-grained soils is applied

418 today in the evaluation of pile capacity. Therefore, two aspects need to be

419 considered as a result of the effects of thermal loads: (i) the possible variation of

420 the pile-soil interface angle of shear strength, which may be approximated as the

421 soil angle of the shear strength under constant volume conditions and (ii) the

422 variation of the normal effective stress acting on the pile shaft, which is associated

423 with volume changes. Most of the research to date has focused on the first aspect.

424 Hueckel and Pellegrini (1989), Hueckel and Baldi (1990), Robinet et al. (1997),

425 Burghignoli et al. (2000), Graham et al. (2001), Cekerevac and Laloui (2004),

426 Ghahremannejad (2003), Yavari et al. (2016), Li et al. (2019), and Maghsoodi et

427 al. (2020) performed studies on clay to assess the angle of shear strength under

428 non-isothermal conditions for different thermal paths. Few studies have been

429 conducted on the thermal effects on the interface shear strength. Recently, Di

430 Donna et al. (2016), Yavari et al. (2016), Li et al. (2019) Yazdani et al. (2019) and

431 Maghsoodi et al. (2020) have performed clay-structure interface tests. Despite

432 some potential variations that turned out to be negligible, all these studies

433   concluded that, from a practical perspective, the angle of shear strength appears to

434   be essentially independent of temperature. When addressing aspect (ii), Di Donna

435   et al. (2016) and Maghsoodi et al. (2020) performed CNS tests at different

436   temperatures where changes in normal stress refer to mechanical shearing. To

437   date, however, no study provides information on the variations of normal stress,

438   referring to variations due solely to thermal cycles which better represents the

439   actual conditions at the pile-soil interface during the operation of the energy

440   foundation.

441   **3.1 Experimental investigation with direct shear tests**

442   The experimental study presented in this paper to investigate the cyclic

443   thermomechanical response of fine-grained soil-concrete interfaces is based on

444   direct shear tests. This test has been recognised as the most representative of the

445   failure mechanism occurring at the pile-soil interface, as it examines both the

446   effects of interface volume changes and the characteristic of surface discontinuity

447   (Boulon and Foray 1986; Boulon 1989; Boulon and Nova 1990; Boulon et al.

448   1995; Ghionna and Mortara 2002; Pra-ai and Boulon 2017). The objective is to

449   provide results for the typical temperature ranges of energy piles where both CNS

450   conditions and cyclic thermal loads are applied simultaneously. These aspects

451   represent the subject matter of this study, as these loading conditions are the most

452   representative of the operation of energy piles and, to date, no results are available

453   in these conditions.

454   **3.1.1 Materials and method**

455   *Materials and sample preparation*

456   The soil used was the same as that used in the oedometric tests. The samples

457   were prepared with the same technique adopted for the oedometric samples, as

458   described above. After compaction, the samples were trimmed down in the direct

459   shear frame with minimal disturbance and were placed in the testing

460   configuration.

461   To perform the interface direct shear tests, a concrete sample was designed and

462   used as the structure. The concrete was prepared in the laboratory in special

463   moulds following the BS EN 206-1:2000 standard; the specifications are shown in

464   Table 3. The roughness of the concrete surface was measured with a Bruker 3D

465   optical microscope (Figure 9). Owing to the size limit of the images, it was not

466   possible to scan the entire surface of the samples. Therefore, special attention was

467   placed on the production of a concrete sample with surface homogeneity. A 12

468   ×12 mm area was subsequently identified as being representative of the entire

469   surface. Image processing involved the analysis of profiles, every 0.4 mm, parallel

470   to the shear direction (x-direction in Figure 9). To determine the roughness of the

471   interface, each profile was divided into a fixed length $L = 0.5$ mm, and the

472   maximum roughness R_{max} was measured at each L. An average R_{max} of 96 μm was

473   obtained, which is within the usual range for concrete surfaces, according to

474   Yoshimi and Kishida (1981).

475   *Equipment*

476   The experimental device adopted in this work was a modified version of the

477   direct shear device produced by GDS instruments described in Di Donna et al.

478   (2016). In the previous version, three main modifications were made to adapt the

479   apparatus to the application of heating episodes at the concrete-soil interface: (i)

the lower part of the shear box, accommodating the concrete sample and heating

system, was redesigned to have a constant contact area between the two materials

and a larger space for installing the thermal system; (ii) the possibility of

imposing CNS conditions was implemented in the GDSLAB software; and (iii) a

heating system composed of an electrical resistance, electrical power supplier,

insulation system, and thermocouples was introduced.

For the present study, further modifications were applied to the direct shear

device to allow the application of cooling episodes to reproduce the in-situ energy

pile-soil interaction on a laboratory scale. First, the lower part of the shear box

was reproduced by opening holes on its wall, through which circulation tubes

were introduced inside. Additionally, a thermal bath was attached to the

circulation tubes to ensure that the circulating water had the target temperatures

and to enable the heating and cooling episodes. For this purpose, the relationship

between the applied temperature, the temperature in the water, and the

temperature inside the cell was carefully determined using a series of

thermocouples (Thermocoax type K, Chromel-Alumel, 2AB 35 DIN, resolution

0.01 °C). During the calibration, thermocouples were inserted into the cell that

was in contact with a sample specifically dedicated to this stage. Four of these

thermocouples were permanently placed in the water container around the cell to

monitor temperature evolution throughout the testing campaign. The shear box

was insulated using polystyrene to minimise heat loss and temperature variations

of the sensors. Horizontal and vertical displacements were measured using two

LVDTs (accuracy 1 μm). Two load cells (maximum vertical force 5 kN, accuracy

0.001 kN) measured the horizontal and vertical loads applied to the sample.

504   During the calibration tests, the same loading paths were applied to steel samples

505   using the same configuration that was applied subsequently in the real tests.

506   Additionally, a water supply system was installed to ensure saturation conditions.

507   The direct shear device, with the new built-in changes, was capable of applying

508   subsequent and multiple heating-cooling cycles to the samples and could thus

509   simulate the actual soil conditions in the vicinity of the energy piles. The modified

510   direct shear device (Figure 10) was used to investigate various conditions related

511   to the field of energy piles.

512   *Experimental program*

513   Preliminary tests were performed under constant normal load (CNL) and CNS

514   conditions for soil-soil and soil-concrete samples under isothermal conditions.

515   However, the main objective of this experimental campaign was to perform tests

516   under non-isothermal conditions in which the samples are subjected to cyclic

517   thermal loads. The goal is to simulate the effects of the operation of the energy

518   piles on the ultimate shear response.

519   In general, the load paths applied were characterised by the following steps: (i)

520   Saturation. (ii) Consolidation under constant mechanical load. In all cases, the

521   samples consisted of clayey soil under NC conditions. (iii) Three thermal cycles

522   (i.e., 5 days) were performed using a heating rate of 2.0 °C/h and a temperature

523   range of $T = 10 \div 40$ °C. Therefore, at this stage, the thermal stress path was

524   analogous to that in the oedometric tests; the only difference was that in this case,

525   to simulate the conditions of volume change at the pile-soil interface more

526   accurately, the third phase was executed under CNS conditions. (iv) Monotonic

527   shearing was performed under CNS conditions at ambient temperature, with an

528   applied strain rate of 0.003 mm/min after the application of cyclic thermal loads.

529   Specifically, for tests conducted under isothermal conditions, the third phase

530   described above was not performed, and the fourth phase was executed under both

531   CNL and CNS conditions. Conventional tests were performed following the

532   specifications of the ASTM D3080/D3080M-11 standard. Table 4 summarises the

533   main variables of all the test performed. Table 5 summarises the initial conditions

534   of the samples. Additionally, Figure 11 shows the stress paths.

535   **3.1.2 Test results**

536   Preliminary tests were performed as reference cases for comparison to better

537   clarify the role of interface, and CNS conditions with respect to the role of

538   temperature for the soil used in these experiments. Therefore, Figure 12 represents

539   a characterisation of the behaviour of the soil and the soil-interface under

540   isothermal conditions. Soil-interface tests in CNS conditions were used as a

541   reference for the test where thermal cycles were applied. The results in Figure 12

542   refers to samples that are NC after the consolidation phase and, consequently, the

543   material do not show any peak. Accordingly, the material contracts during the

544   shear tests. Similar results were obtained by Di Donna et al. (2016) when

545   comparing the soil-soil (Test 4) and soil-concrete (Test 6) test profiles under CNL

546   conditions, where soil failure was assumed to occur. The comparison of the soil-

547   concrete test profiles under CNL and CNS conditions (i.e., Tests 6 and 7,

548   respectively) is similar to the behaviour of a loose sand/smooth interface

549   observed, for instance, by Porcino et al. (2003). A reduction in maximum shear

550   stress can be observed with an increase in the stiffness. Simultaneously, the

551   increase in normal stiffness causes a reduction in the current normal stress. The

552 above effects can be correlated with the contractive behaviour exhibited by the

553 material. A contraction yields to a decrease of the current normal stress,

554 corresponding to a decrease of the shear stress, as a consequence of the elastic

555 constraint provided by the soil surrounding the interface.

556   Figure 13 shows four clay-concrete interface tests performed under CNS

557 conditions. Tests 7 and 9 refer to a standard CNS direct shear test in which a

558 purely mechanical stress path is applied. For these tests, the third step described

559 earlier was not performed. The results of the shearing phase, following the cyclic

560 thermal loads, are represented by Tests 8 and 10. Notably, the application of

561 thermal loads has a negligible effect on shear stress in the shearing phase. The

562 variations in the shear strength angles are minimal and are not crucial in the

563 definition of the failure envelope, which remains practically unaffected (Figure

564 14). Some differences in the axial displacement are attributed to the effect of time

565 because, in Tests 8 and 10, shearing occurs after the thermal cycles (i.e., 7 days),

566 and minor importance is attributed to the cyclic thermal consolidation. Volume

567 changes when applying thermal loads under CNS conditions are in the order of

568 magnitude of those measured during the oedometric tests (Figure 15). The non-

569 linear behaviour of the device at this test stage makes precise quantification

570 difficult. However, with almost no effect, it is possible to assume that the volume

571 change is not significant for the shear resistance under the investigated conditions

572 (i.e., there are no significant changes in the effective normal stress during the

573 thermal cycle as shown in Figure 15).

574   Additionally, the failure mechanism of the soil-structure interface within the

575   framework of elastoplasticity is discussed by Ravera and Laloui (2020)[1], and a

576   constitutive model applicable to both conventional and energy piles is described.

577

578   **4. Conclusion**

579   The cyclic thermomechanical behaviour of the soil-concrete interface was

580   investigated by performing a testing programme including cyclic thermal tests

581   under constant vertical effective stress in oedometric conditions, and CNS

582   interface direct shear tests, where the samples have been subjected to thermal

583   cycles. The main objective was to experimentally analyse the soil-concrete

584   interface failure mechanism of energy piles. The shear behaviour of the soil-pile

585   interface is characterised by large localised strains concentrated in a thin layer

586   around the pile, i.e., the interface zone, surrounded by soil behaving in oedometric

587   conditions. The tests conducted allowed the volumetric and shear aspects that

588   characterise the failure mechanism to be analysed first separately and then in

589   combination.

590   The framework proposed here provides answers on how the soil-concrete

591   interface responds to thermal and mechanical loads, which is useful for solving

592   geotechnical problems. This study extrapolates information of interest (e.g.,

593   consolidation behaviour and failure envelopes) to an engineering application such

594   as energy piles.

---

[1] Ravera, E., and Laloui, L. 2020. Failure mechanism of soil-structure interface for energy piles. Canadian Geotechnical Journal. *(under review)*.

595   The results of the thermovolumetric behaviour study show very low residual

596   strain variations towards cyclic thermal variations. This means that the boundary

597   conditions of the interface zone are not altered by the temperature cycle. In

598   addition, this section presents an interpretation procedure based on the mechanical

599   analogy with the advantage of analysing the effects of mechanical and thermal

600   loads for an energy pile design according to the classical scheme of geotechnical

601   analysis. The presented procedure can provide a basis for the development of new

602   testing standards. Presently, the lack of standards and interpretation procedures is

603   one of the major issues that hinder the extension of this technology from academia

604   to industry. Therefore, the development of testing methods and equipment

605   designed for engineering purposes can facilitate the spread of this technology.

606   The main interest in analysing the pile-soil interface behaviour is associated with

607   the fact that the greater the volume variation under cyclic loads, the greater the

608   probability of shear resistance degradation (i.e., reduction of normal stress). For

609   this purpose, a direct shear test device was modified to enable the application of

610   heating-cooling cycles under CNS conditions. The results of this study show that

611   the probability of pile shear resistance degradation, when subjected to a thermal

612   cyclic load is minimal and that changes in the failure envelope are negligible.

613   With these insignificant effects, volume change does not appear to be decisive in

614   affecting shear resistance (i.e., there are no significant variations in effective

615   normal stress during a thermal cycle).

616   It is acknowledged that the results are valid for the sequence of the applied

617   heating and cooling cycles in this study. The relevance of these observations in

618 the event that the cooling cycle precedes the one of heating requires further

619 investigation.

620   Based on these results, it is possible to make some considerations for the

621 analysis and design of energy piles. From a practical perspective, the results show

622 an almost reversible volumetric behaviour and negligible effects on shear strength

623 of the soil-concrete interface towards cyclic thermal loads. Thus, neglecting

624 temperature sensitivity may be justified, as when simplified analysis methods are

625 used in the preliminary design stages.

626 Acknowledgements

629

References

Abuel-Naga, H. M., Bergado, D. T., and Bouazza, A. 2007. Thermally induced volume change and excess pore water pressure of soft Bangkok clay. Engineering Geology, **89**(1-2), 144-154.

ASTM D2435/2435M-11. 2011. Standard Test Methods for One-Dimensional Consolidation Properties of Soils Using Incremental Loading. ASTM International, West Conshohocken, PA

ASTM. D3080/D3080M-11. 2011. Standard test method for direct shear test of soils under consolidated drained conditions. ASTM International, West Conshohocken, PA

Baldi, G., Hueckel, T., Peano, A., and Pellegrini, R. 1991. Developments in modelling of thermohydro-geomechanical behaviour of Boom clay and clay-based buffer materials (Volume 1) (No. EUR--13365/1). Commission of the European Communities.

Boulon, M. 1989. Basic features of soil structure interface behaviour. Computers and Geotechnics, **7**(1-2), 115-131.

Boulon, M., and Foray, P. 1986. Physical and numerical simulation of lateral shaft friction along offshore piles in sand. In Proc., 3rd Int. Conf. on Numerical methods in offshore piling (pp. 127-147). Nantes, France: Institut Francais du Petrol.

Boulon, M., and Nova, R. 1990. Modelling of soil-structure interface behaviour a comparison between elastoplastic and rate type laws. Computers and Geotechnics, **9**(1-2), 21-46.

Boulon, M., Garnica, P., and Vermeer, P. A. 1995. Soil-structure interaction: FEM computations. Studies in Applied Mechanics, **42**, 147-147.

Burghignoli, A., Desideri, A., and Miliziano, S. 2000. A laboratory study on the thermomechanical behaviour of clayey soils. Canadian Geotechnical Journal, **37**(4), 764-780.

Campanella, R. G., and Mitchell, J. K. 1968. Influence of temperature variations on soil behavior. Journal of Soil Mechanics and Foundations Div.

Cekerevac, C., and Laloui, L. 2004. Experimental study of thermal effects on the mechanical behaviour of a clay. International journal for numerical and analytical methods in geomechanics, **28**(3), 209-228.

Coccia, C. J. R., and McCartney, J. S. 2016. Thermal volume change of poorly draining soils I: critical assessment of volume change mechanisms. Computers and Geotechnics, **80**, 26-40.

Di Donna, A., and Laloui, L. 2015. Response of soil subjected to thermal cyclic loading: experimental and constitutive study. Engineering Geology, **190**, 65-76.

Di Donna, A., Ferrari, A., and Laloui, L. 2016. Experimental investigations of the soil–concrete interface: physical mechanisms, cyclic mobilization, and behaviour at different temperatures. Canadian Geotechnical Journal, **53**(4), 659-672.

EN, B. (2001). 206-1: 2000. Concrete, Specification, Performance, Production and Conformity.

Fakharian, K., and Evgin, E. 1997. Cyclic simple-shear behavior of sand-steel interfaces under constant normal stiffness condition. Journal of Geotechnical and Geoenvironmental Engineering, **123**(12), 1096-1105.

Finn, F. 1952, January. The effect of temperature on the consolidation characteristics of remolded clay. In Symposium on Consolidation Testing of Soils. ASTM International.

Fleureau, J.M. 1979. Influence d'un champ thermique ou électrique sur les phénomènes d'interaction solide-liquide dans le milieux poreux. Ph.D. Thesis. École Centrale Paris.

Ghahremannejad, B. 2003. Thermo-mechanical behaviour of two reconstituted clays. Ph. D Thesis

Ghionna, V. N., and Mortara, G. 2002. An elastoplastic model for sand–structure interface behaviour. Géotechnique, **52**(1), 41-50.

Graham, J., Tanaka, N., Crilly, T., and Alfaro, M. 2001. Modified Cam-Clay modelling of temperature effects in clays. Canadian geotechnical journal, **38**(3), 608-621.

Hueckel, T., and Baldi, G. 1990. Thermoplasticity of saturated clays: experimental constitutive study. Journal of geotechnical engineering, **116**(12), 1778-1796.

Hueckel, T., and Pellegrini, R. 1989. Modeling of thermal failure of saturated clays. In International symposium on numerical models in geomechanics. 3 (NUMOG III) (pp. 81-90).

Hueckel, T., and Pellegrini, R. 1996. A note on thermomechanical anisotropy of clays. Engineering geology, **41**(1-4), 171-180.

Hueckel, T., François, B., and Laloui, L. 2009. Explaining thermal failure in saturated clays. Géotechnique, **59**(3), 197-212.

Kingery, W.D., Bowen, H.K., and Uhlmann, D.R. 1976. Introduction to Ceramics. 2nd Edition Wiley.

Laloui, L. 2001. Thermomechanical behaviour of soils. Environmental Geomechanics, EPFL Press, 809-843.

Laloui, L., and Cekerevac, C. 2003. Thermo-plasticity of clays: an isotropic yield mechanism. Computers and Geotechnics, **30**(8), 649-660.

Laloui, L., and Rotta Loria, A. F. 2019. Analysis and Design of Energy Geostructures: Theoretical Essentials and Practical Application. Academic Press.

Laloui, L., Leroueil, S., and Chalindar, S. 2008. Modelling the combined effect of strain rate and temperature on one-dimensional compression of soils. Canadian Geotechnical Journal, **45**(12), 1765-1777.

Laloui L., François B., Nuth M., Péron H. and Koliji, A. 2008. A thermo-hydro-mechanical stress-strain framework for modeling the performance of clay barriers in deep geological repositories for radioactive waste. In Unsaturated Soils: Advances in Geo-Engineering, 63-80. Toll et al. (eds).

Laloui, L., Olgun, C. G., Sutman, M., McCartney, J. S., Coccia, C. J., Abuel-Naga, H. M., and Bowers, G. A. 2014. Issues involved with thermoactive geotechnical systems: Characterization of thermomechanical soil behavior and soil-structure interface behavior. DFI Journal-The Journal of the Deep Foundations Institute, **8**(2), 108-120.

Leroueil, S. 1996. Importance of strain rate and temperature effects in geotechnical engineering. Measuring and modeling time dependent soil behavior. ASCE, 1-60.

Li, C., Kong, G., Liu, H., and Abuel-Naga, H. 2019. Effect of temperature on behaviour of red clay–structure interface. Canadian Geotechnical Journal, **56**(1), 126-134.

Maghsoodi, S., Cuisinier, O., and Masrouri, F. 2020. Thermal effects on mechanical behaviour of soil–structure interface. Canadian Geotechnical Journal, **57**(1), 32-47.

McCartney, J. S., Jafari, N. H., Hueckel, T., Sánchez, M., and Vahedifard, F. 2019. Emerging thermal issues in geotechnical engineering. In Geotechnical fundamentals for addressing new world challenges (pp. 275-317). Springer, Cham.

Mimouni, T. and Laloui, L. 2015. Behaviour of a group of energy piles. Canadian Geotechnical Journal **52**, No. 12, 1913–1929.

Mitchell, J. K., and Soga, K. 2005. Fundamentals of soil behavior (Vol. 3). New York: John Wiley & Sons.

Plum, R.L. and Esrig, M. I. 1969. Some temperature effects on soil compressibility and pore water pressure. Special Report, (103), 231.

Porcino, D., Fioravante, V., Ghionna, V. N., and Pedroni, S. 2003. Interface behavior of sands from constant normal stiffness direct shear tests. Geotechnical Testing Journal, **26**(3), 289-301.

Pra-ai, S., and Boulon, M. 2017. Soil–structure cyclic direct shear tests: a new interpretation of the direct shear experiment and its application to a series of cyclic tests. Acta Geotechnica, **12**(1), 107-127.

Pusch, R. 1986. Permanent crystal lattice contraction, a primary mechanism in thermally induced alteration of Na Bentonite. In MRS Online Proceedings Library, vol 84.

Ravera, E., Sutman, M., and Laloui, L. 2020a. Analysis of the interaction factor method for energy pile groups with slab. Computers and Geotechnics, **119**, 103294.

Ravera, E., Sutman, M., and Laloui, L. 2020b. Load Transfer Method for Energy Piles in a Group with Pile–Soil–Slab–Pile Interaction. Journal of Geotechnical and Geoenvironmental Engineering, **146**(6), 04020042.

Robinet, J. C., Pasquiou, A., Jullien, A., Belanteur, N., and Plas, F. 1997. Expériences de laboratoire sur le comportement thermo-hydro-mécanique de matériaux argileux remaniés gonflants et non gonflants. Revue française de géotechnique, **81**, 53-80.

Romero Morales, E. E. 1999. Characterisation and thermo-hydro-mechanical behaviour of unsaturated Boom clay: an experimental study. Universitat Politècnica de Catalunya.

Rotta Loria, A. F., and Coulibaly, J. B. 2020. Thermally induced deformation of soils: A critical overview of phenomena, challenges and opportunities. Geomechanics for Energy and the Environment, 100193.

Rotta Loria, A. F., and L. Laloui. 2016. The interaction factor method for energy pile groups. Computers and Geotechnics. **80** (Dec): 121–137.

Rotta Loria, A. F. and Laloui, L. 2017a. Thermally induced group effects among energy piles. Géotechnique **67** (5), 374-393

Rotta Loria, A. F., and L. Laloui. 2017b. The equivalent pier method for energy pile groups. Géotechnique **67** (8): 691–702.

Shetty, R., Singh, D. N., and Ferrari, A. 2019. Volume change characteristics of fine-grained soils due to sequential thermo-mechanical stresses. Engineering Geology, **253**, 47-54.

Sutman, M. 2016. Thermo-mechanical behavior of energy piles: Full-scale field testing and numerical modeling. PhD thesis, Virginia Tech.

Sutman, M., Olgun, C.G. and Laloui, L. 2019. Cyclic load–transfer approach for the analysis of energy piles. Journal of Geotechnical and Geoenvironmental Engineering, **145**(1), p.04018101.

Tabucanon, J. T., Airey, D. W., and Poulos, H. G. 1995. Pile skin friction in sands from constant normal stiffness tests. Geotechnical Testing Journal, **18**(3), 350-364.

Towhata, I., Kuntiwattanaku, P., Seko, I., and Ohishi, K. 1993. Volume change of clays induced by heating as observed in consolidation tests. Soils and Foundations, **33**(4), 170-183.

Vega, A., Coccia, C. J., El Tawati, A., and McCartney, J. S. 2012. Impact of the rate of heating on the thermal consolidation of saturated silt. In GeoCongress 2012: State of the Art and Practice in Geotechnical Engineering (pp. 4476-4485).

Yavari, N., Tang, A. M., Pereira, J. M., and Hassen, G. 2016. Effect of temperature on the shear strength of soils and the soil–structure interface. Canadian Geotechnical Journal, **53**(7), 1186-1194.

Yoshimi, Y., and Kishida, T. 1981. A ring torsion apparatus for evaluating friction between soil and metal surfaces. Geotechnical testing journal, **4**(4), 145-152.

Table 1. Thermal cycle oedometer: test variables

Test N°	Label	Sample N°	OCR	Confining pressure [kPa]	Rate of heating [°C/h]	T range [°C]	ΔT [°C]	N° of cycles
0	SO	S0 S0bis	-	0÷1000	-	-	-	-
1	TO_NC_125	S1 S1bis	1	125	2	10÷40	+20/-10	5
2	TO_NC_1000	S2 S2bis	1	1000	2	10÷40	+20/-10	2
3	TO_OC_125	S3 S3bis	2	125	2	10÷40	+20/-10	2

Table 2. Thermal cycle oedometer: initial conditions of the samples

Test N°	Sample N°	w [%]	e [-]	ρ_s [Mg/m^3]	ρ [Mg/m^3]
0	S0	35.2	1.405	2.65	1.49
	S0bis	35.2	1.404	2.65	1.49
1	S1	35.7	1.410	2.65	1.49
	S1bis	35.7	1.421	2.65	1.49
2	S2	35.2	1.418	2.65	1.48
	S2bis	35.2	1.416	2.65	1.48
3	S3	35.1	1.414	2.65	1.48
	S3bis	35.1	1.415	2.65	1.48

Table 3. Concrete mix design

Concrete mix design	BS EN 206-1:2000
Cement	
Aggregate	0-16 mm
Water/cement	0.6
Aggregate/cement	6

Table 4. Direct shear tests: test variables

Test N°	Label	Sample N°	OCR	Initial normal stress [kPa]	Shear condition	Rate of shearing [mm/min]	ΔT [°C]	N° of cycles
4	SS_CNL_125	S4	1	125	CNL K=0 kPa/mm	0.003	-	-
5	SS_CNS_125	S5	1	125	CNS K=200 kPa/mm	0.003	-	-
6	SC_CNL_125	S6	1	125	CNL K=0 kPa/mm	0.003	-	-
7	SC_CNS_125	S7	1	125	CNS K=200 kPa/mm	0.003	-	-
8	SC_CNS_125_T	S8	1	125	CNS K=200 kPa/mm	0.003	+20/-10	3
9	SC_CNS_250	S9	1	250	CNS K=200 kPa/mm	0.003	-	-
10	SC_CNS_250_T	S10	1	250	CNS K=200 kPa/mm	0.003	+20/-10	3

Table 5. Direct shear tests: initial conditions of the samples

Test N°	Sample N°	w [%]	e [-]	ρ_s [Mg/m^3]	ρ [Mg/m^3]
4	S4	35.8	1.400	2.65	1.50
5	S5	36.3	1.400	2.65	1.50
6	S6	35.6	1.400	2.65	1.50
7	S7	36.2	1.400	2.65	1.50
8	S8	34.6	1.400	2.65	1.49
9	S9	34.5	1.400	2.65	1.49
10	S10	35.5	1.400	2.65	1.50

List of figures

Figure 1. Schematic representation of the failure mechanism that occurs at the pile interface: (a) large localised strains are concentrated in a thin layer around the pile, i.e., the interface, (b) modelling approach of the interface zone, and (c) interface failure mechanism, where a shear band is detached from the surrounding soil that behaves in oedometric conditions, reproduced in the laboratory. (u and w are the axial and shear displacement respectively; σ and τ are the normal and shear stress respectively; K is the spring stiffness)

Figure 2. Particle size distribution of the clayey soil used in the experiments. Atterberg's limits: liquid limit 56 %, plastic limit 32%, plasticity index 24%. Mineralogical composition: 77% illite, 10% kaolinite, 12% calcite, and traces of feldspar and quartz

Figure 3. Temperature-controlled oedometric cell: (a) global view of the system (1: software control and datalogger thermocouples, 2: thermal bath, 3: thermocouples, 4: insulation, 5: thermal hydraulic system, and 6: water supply system). (b) schematic representation of the temperature-controlled oedometric cell

Figure 4. Oedometer thermomechanical paths. Heating-cooling cycles at constant vertical effective stress for normally consolidated clayey samples (Tests 1 and 2) and overconsolidated clayey samples (Test 3)

Figure 5. Interpretation procedure for thermal load and temperature evolution measured over time for normally consolidated clayey samples (Test 1). Analysis of the relative role of primary consolidation and secondary compression in the volumetric response of fine-grained soils. Positive displacements represent expansion and negative displacements represent contraction

Figure 6. Interpretation procedure for thermal load and temperature evolution measured over time for overconsolidated clayey samples (Test 3). Analysis of the relative role of primary consolidation and secondary compression in the volumetric response of fine-grained soils. Positive displacements represent expansion and negative displacements represent contraction

Figure 7. Standard oedometer tests results of clayey samples in terms of axial strain

Figure 8. Volumetric behaviour of fine-grained soils subjected to thermal cycles. Heating and cooling of (a) normally consolidated clayey samples at a constant vertical effective stress of 125 kPa; (b) normally consolidated clayey samples at a constant vertical effective stress of 1000 kPa, and (c) overconsolidated clayey samples at a constant vertical stress of 125 kPa

Figure 9. Determination of concrete roughness by optical microscope: (a) image of the concrete surface acquired by a Bruker 3D optical microscope, (b) examples of roughness profiles for two specific sections, and (c) photograph of the concrete surface

Figure 10. Modified direct shear device: (a) global view of the system (1: software control, 2: datalogger thermocouples, 3: insulation, 4: thermal bath, and 5: water supply system). (b) and (c) details of the modified shear box. (d) and (e) schematic representation of the shear box

Figure 11. Stress-temperature paths followed during direct shear tests. Tests 4 and 6: path 0-1-2; Tests 5, 7, and 9: path 0-1-3; Tests 8 and 10: path 0-1-4-3

Figure 12. Clay-clay and clay-concrete interface tests under isothermal conditions. (a) stress-strain behaviour; (b) Mohr plane: load paths and failure behaviour; (c) dilatancy effects, and (d) volumetric behaviour

Figure 13. Clay-concrete interface tests under CNS conditions: (solid) being subjected to thermal cycles, (dash) not subjected to thermal cycles. (a) stress-strain behaviour; (b) Mohr plane: load paths and failure behaviour; (c) dilatancy effects, and (d) volumetric behaviour
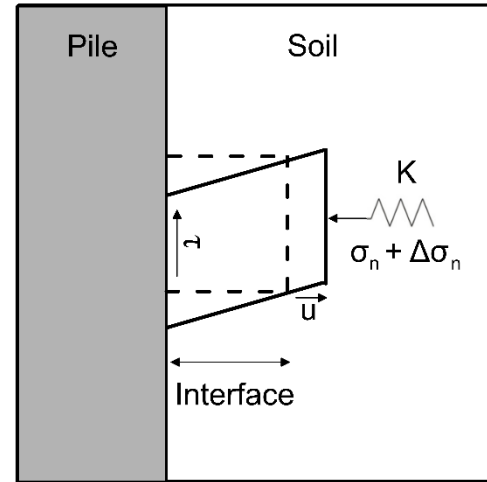
Figure 14. Clay-concrete interface failure envelopes for testing under CNS conditions: (black) being subjected to thermal cycles, (grey) not subjected to thermal cycles

Figure 15. (a) Comparison between measured axial strain under CNL and CNS conditions during a heating-cooling cycle. (b) Measured normal effective stress variation during a heating-cooling thermal cycle

(a) In situ conditions

(b) Detail

Pile | Soil

$\sigma_n + \Delta\sigma_n$

K

Interface

(c) Laboratory conditions

$\sigma_n + \Delta\sigma_n$ K

u

Oedometer part

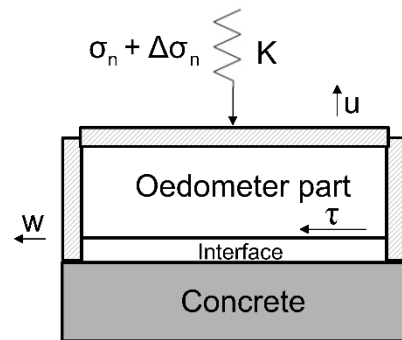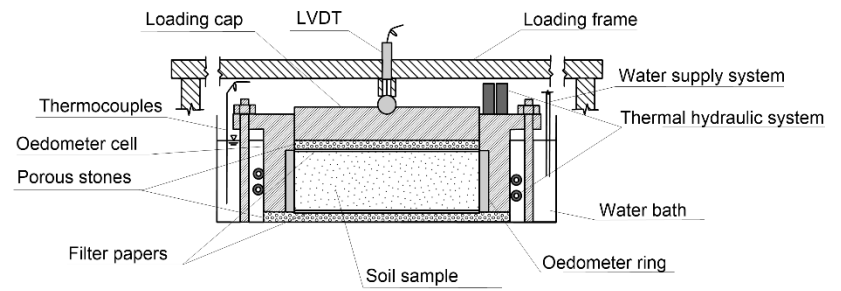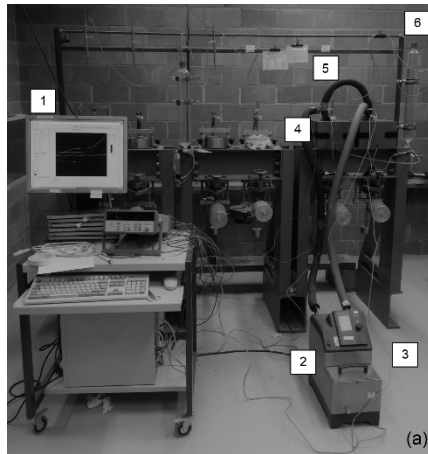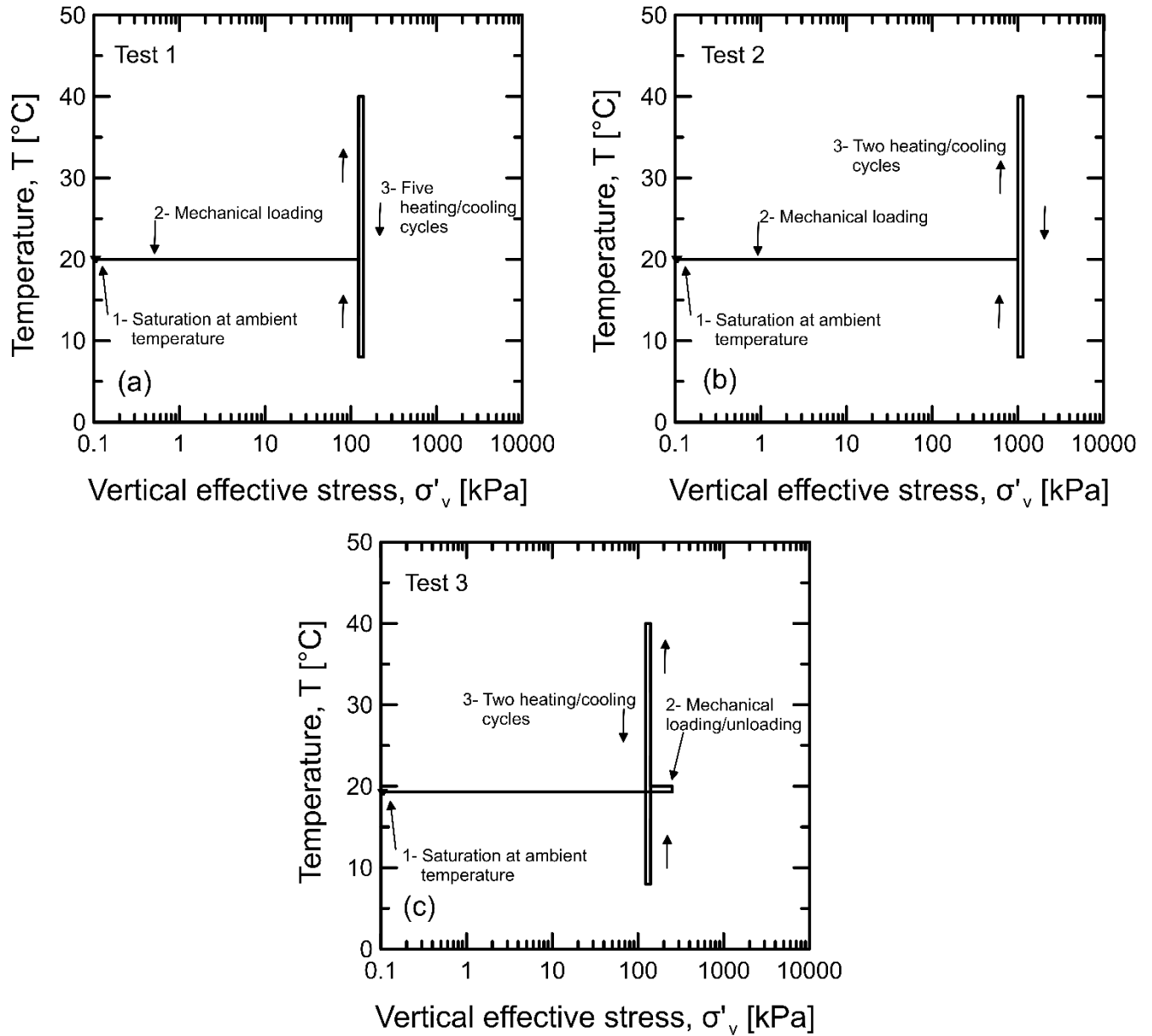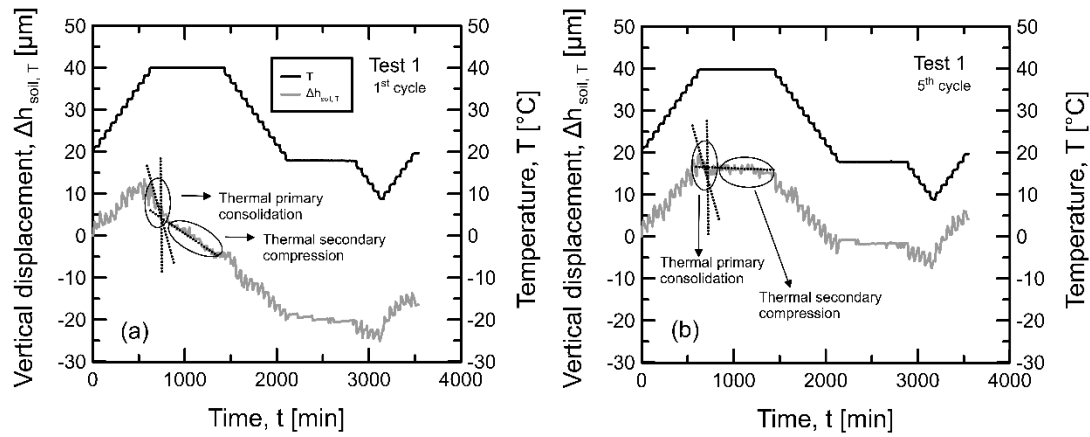τ

w

Interface

Concrete

Figure 1. Schematic representation of the failure mechanism that occurs at the pile interface: (a) large localised strains are concentrated in a thin layer around the pile, i.e., the interface, (b) modelling approach of the interface zone, and (c) interface failure mechanism, where a shear band is detached from the surrounding soil that behaves in oedometric conditions, reproduced in the laboratory. (u and w are the axial and shear displacement respectively; σ and τ are the normal and shear stress respectively; K is the spring stiffness)

Figure 2. Particle size distribution of the clayey soil used in the experiments. Atterberg's limits: liquid limit 56 %, plastic limit 32%, plasticity index 24%. Mineralogical composition: 77% illite, 10% kaolinite, 12% calcite, and traces of feldspar and quartz

Figure 3. Temperature-controlled oedometric cell: (a) global view of the system (1: software control and datalogger thermocouples, 2: thermal bath, 3: thermocouples, 4: insulation, 5: thermal hydraulic system, and 6: water supply system). (b) schematic representation of the temperature-controlled oedometric cell

Figure 4. Oedometer thermomechanical paths. Heating-cooling cycles at constant vertical effective stress for normally consolidated clayey samples (Tests 1 and 2) and overconsolidated clayey samples (Test 3)

Figure 5. Interpretation procedure for thermal load and temperature evolution measured over time for normally consolidated clayey samples (Test 1). Analysis of the relative role of primary consolidation and secondary compression in the volumetric response of fine-grained soils. Positive displacements represent expansion and negative displacements represent contraction

Figure 6. Interpretation procedure for thermal load and temperature evolution measured over time for overconsolidated clayey samples (Test 3). Analysis of the relative role of primary consolidation and secondary compression in the volumetric response of fine-grained soils. Positive displacements represent expansion and negative displacements represent contraction

Figure 7. Standard oedometer tests results of clayey samples in terms of axial strain

Figure 8. Volumetric behaviour of fine-grained soils subjected to thermal cycles. Heating and cooling of (a) normally consolidated clayey samples at a constant vertical effective stress of 125 kPa; (b) normally consolidated clayey samples at a constant vertical effective stress of 1000 kPa, and (c) overconsolidated clayey samples at a constant vertical stress of 125 kPa
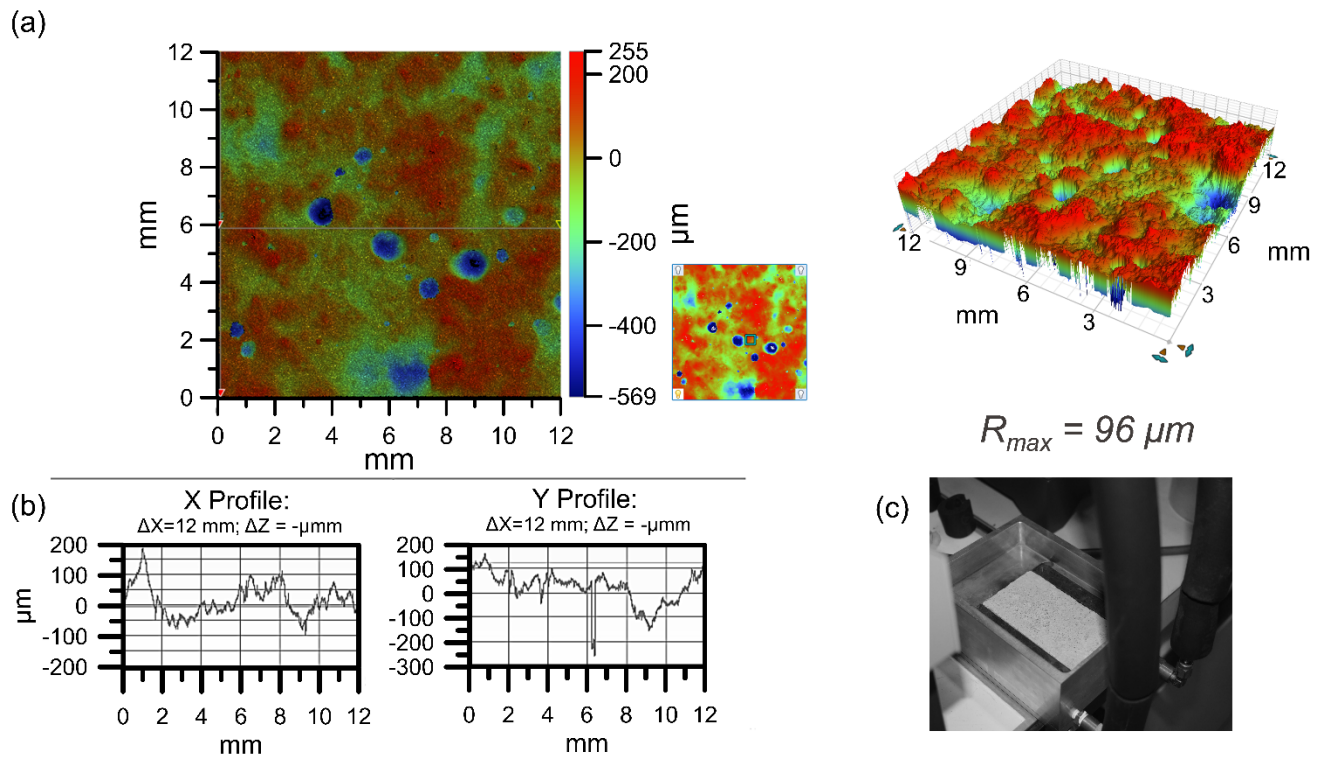
Figure 9. Determination of concrete roughness by optical microscope: (a) image of the concrete surface acquired by a Bruker 3D optical microscope, (b) examples of roughness profiles for two specific sections, and (c) photograph of the concrete surface

Figure 10. Modified direct shear device: (a) global view of the system (1: software control, 2: datalogger thermocouples, 3: insulation, 4: thermal bath, and 5: water supply system). (b) and (c) details of the modified shear box. (d) and (e) schematic representation of the shear box

Figure 11. Stress-temperature paths followed during direct shear tests. Tests 4 and 6: path 0-1-2; Tests 5, 7, and 9: path 0-1-3; Tests 8 and 10: path 0-1-4-3
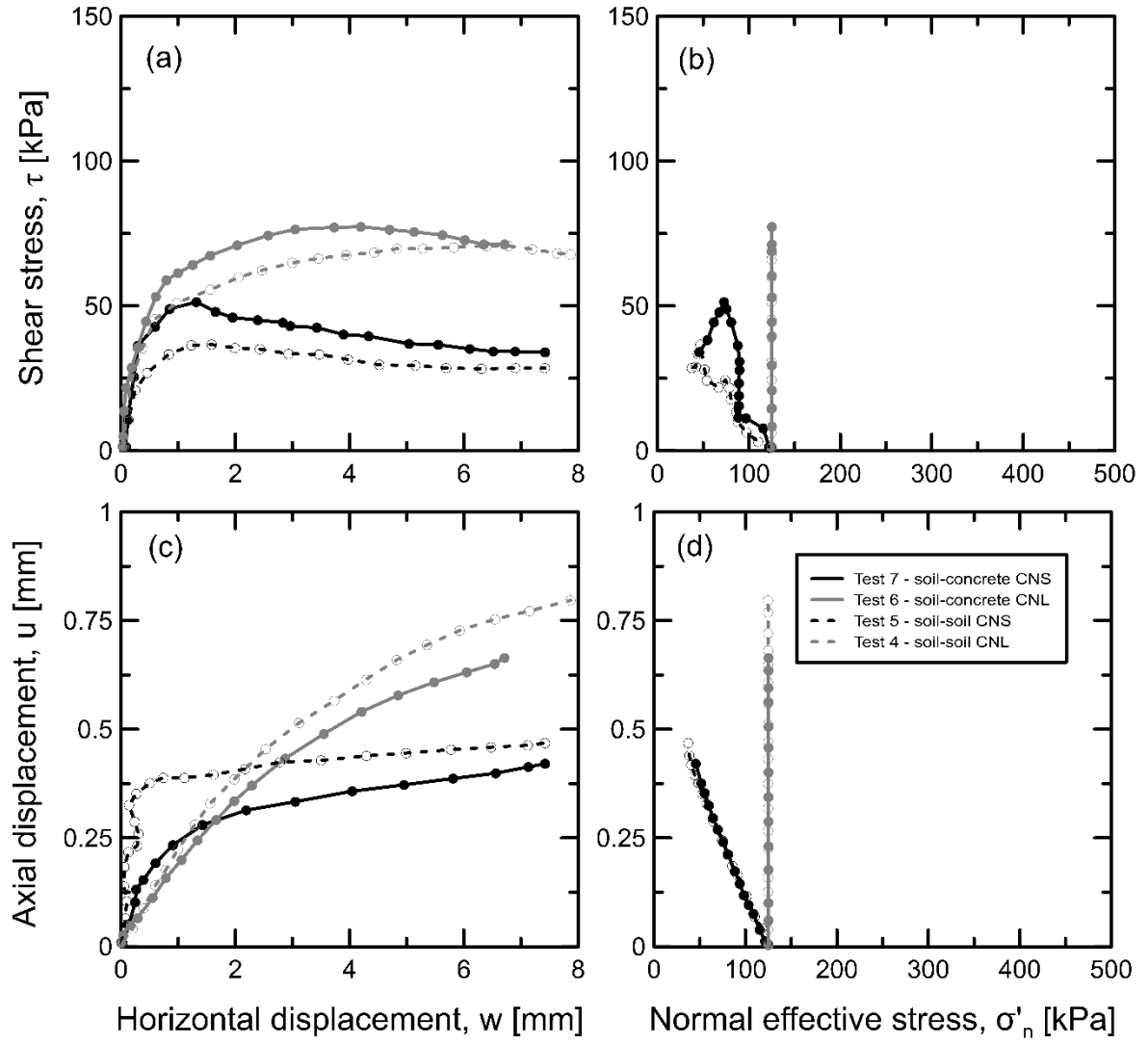
Figure 12. Clay-clay and clay-concrete interface tests under isothermal conditions. (a) stress-strain behaviour; (b) Mohr plane: load paths and failure behaviour; (c) dilatancy effects, and (d) volumetric behaviour
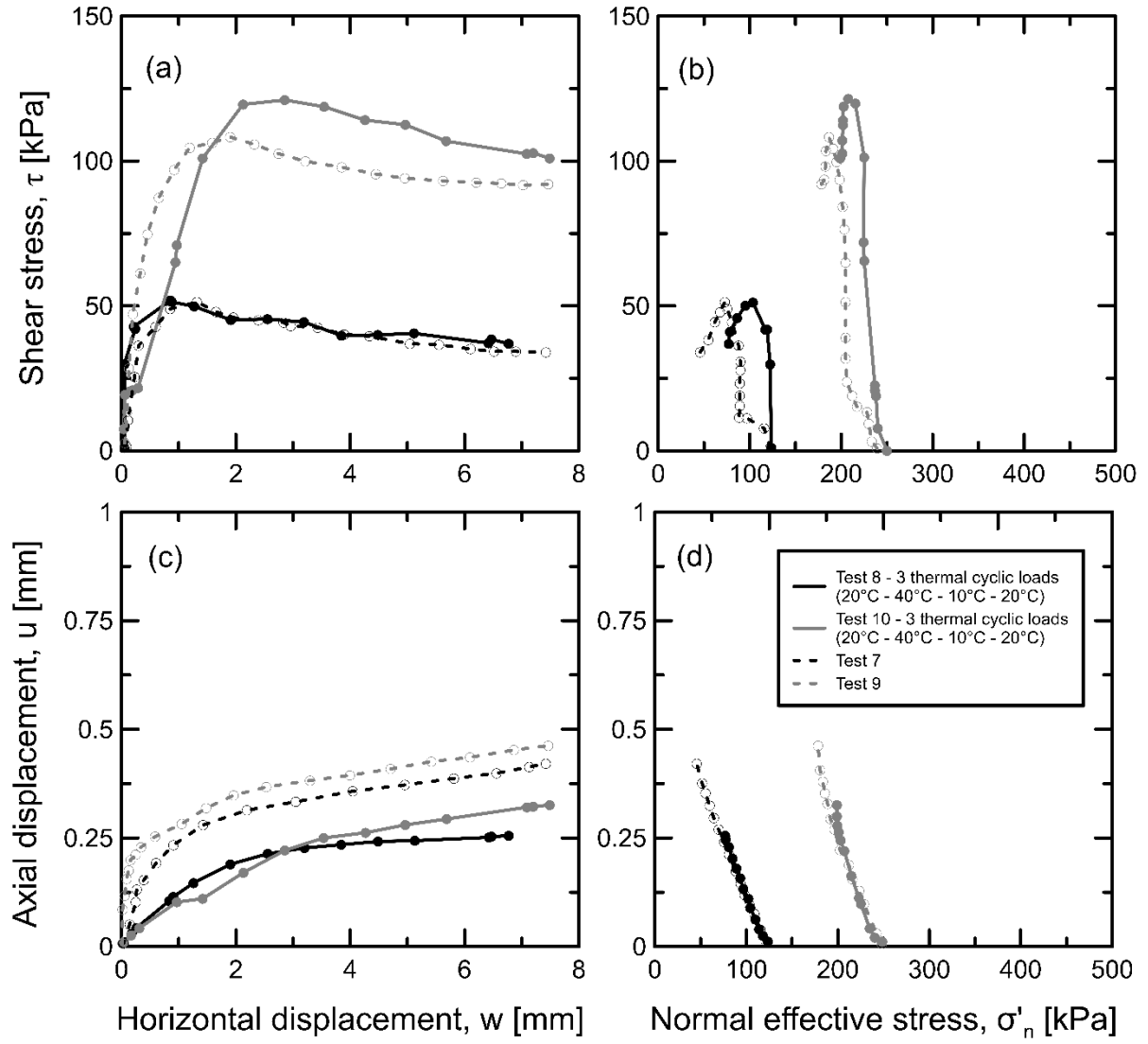
Figure 13. Clay-concrete interface tests under CNS conditions: (solid) being subjected to thermal cycles, (dash) not subjected to thermal cycles. (a) stress-strain behaviour; (b) Mohr plane: load paths and failure behaviour; (c) dilatancy effects, and (d) volumetric behaviour
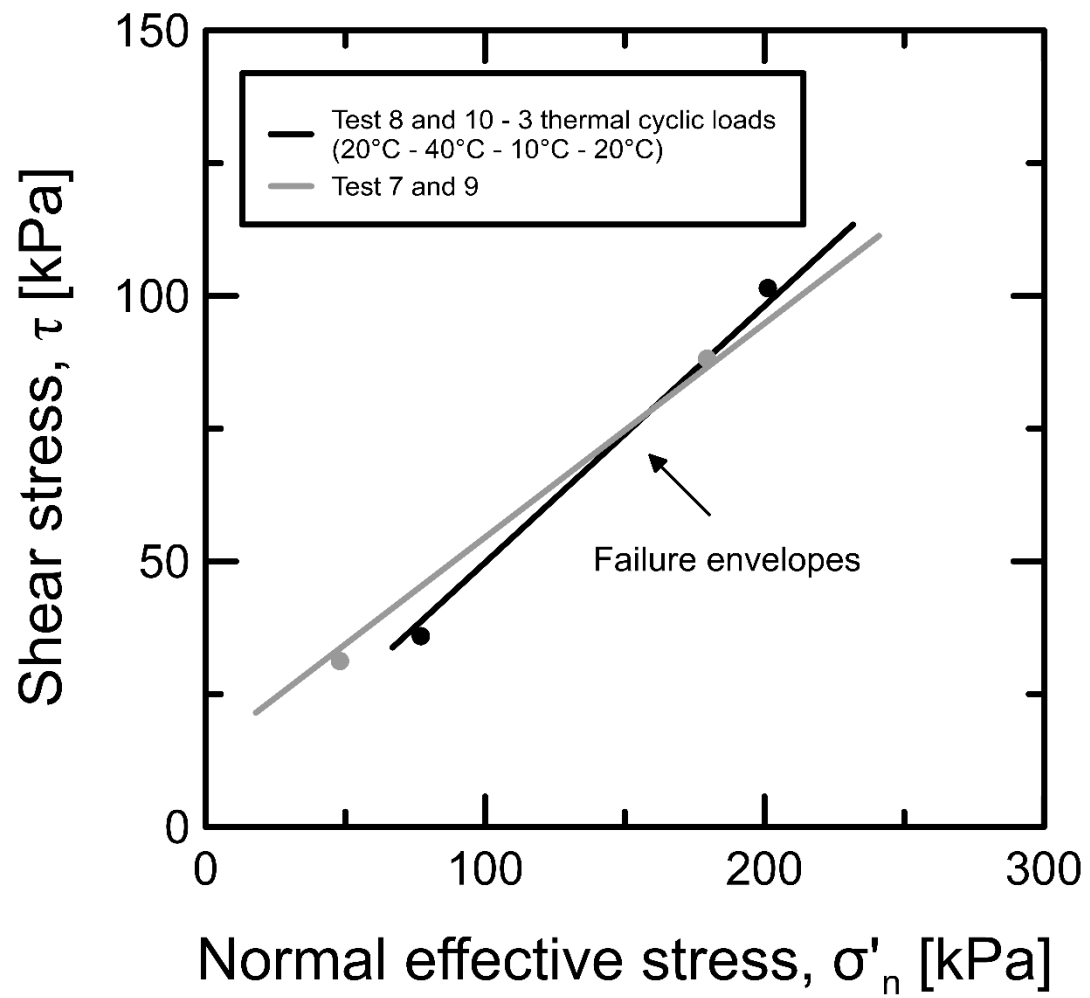
Figure 14. Clay-concrete interface failure envelopes for testing under CNS conditions: (black) being subjected to thermal cycles, (grey) not subjected to thermal cycles
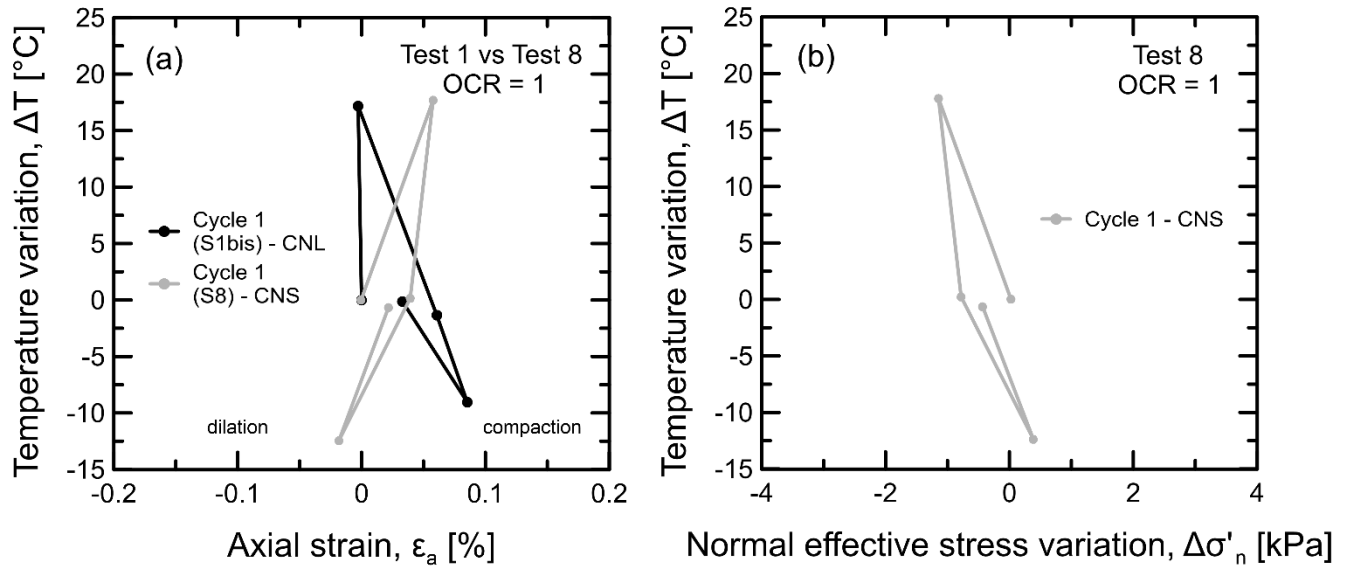
Figure 15. (a) Comparison between measured axial strain under CNL and CNS conditions during a heating-cooling cycle. (b) Measured normal effective stress variation during a heating-cooling thermal cycle